Honda K, Okusaka T, Felix K, Nakamori S, et. al.	Altered plasma apolipoprotein modifications in patients with pancreatic cancer: protein characterization and multi-institutional validation.	PLoS One	7(10)	e46908	2012
Mayahara H, Ito Y, Morizane C, Ueno H, Okusaka T, et. al.	Salvage chemoradiotherapy after primary chemotherapy for locally advanced pancreatic cancer: a single-institution retrospective analysis.	BMC Cancer	12	609	2012
Ueno H, Ioka T, Ikeda M, Okusaka T , et. al.	Randomized phase III study of gemcitabine plus S-1, S-1 alone, or gemcitabine alone in patients with locally advanced and metastatic pancreatic cancer in Japan and Taiwan: GEST study.	J Clin Oncol	31(13)	1640-8	2013
Ikeda M, Ioka T, Ito Y, Yonemoto N, Okusaka T, et. al.	A multicenter phase II trial of S-1 with concurrent radiation therapy for locally advanced pancreatic cancer.	Int J Radiat Oncol Biol Phys	85(1)	163-9	2013
Furuse J, Ishii H, Okusaka T	The Hepatobiliary and Pancreatic Oncology (HBPO) Group of the Japan Clinical Oncology Group (JCOG): history and future direction.	Jpn J Clin Oncol	43(1)	2-7	2013
Suzuki E, Ikeda M, Okusaka T, Nakamori S, et. al.	A multicenter phase II study of S-1 for gemcitabine-refractory biliary tract cancer.	Cancer Chemother Pharmacol	71(5)	1141-6	2013
Umemura S, Mimaki S, Makinoshima H, Tada S, et. al.	Therapeutic priority of the PI3K/AKT/mTOR pathway in small cell lung cancers as revealed by a comprehensive genomic analysis.	Journal of Thoracic Oncology	9	1324-31	2014

Takeda A, Fujii H, et. al.	Maximum Standardized Uptake Value on FDG-PET is a Strong Predictor of Overall and Disease-Free Survival for Non-Small-Cell Lung Cancer Patients after Stereotactic Body Radiotherapy	J Thorac Oncol	9 (1)	65-73	2014
Yoshimoto M, Hayakawa T, Mutoh M, Fujii H, et. al.	In vivo SPECT imaging with ^{111}In-DOTA-c(RGDfK) to detect early pancreatic cancer in a hamster pancreatic carcinogenesis model.	J Nucl Med	53(5)	765-71	2012
Fujii H, Yamaguchi M, Inoue K, Mutou Y, et. al.	In vivo visualization of heterogeneous intratumoral distribution of hypoxia-inducible factor-1α activity by the fusion of high-resolution SPECT and morphological imaging tests.	J Biomed Biotechnol	2012	262741	2012
Kaburagi T, Takeuchi H, Fujii H, Saikawa Y, et. al.	Initial experience of individualized chemoradiotherapy for superficial esophageal cancers based on the sentinel lymph node concept.	Esophagus	9(3)	147-152	2012
Takeda A, Kunieda E, Fujii H, Yokosuka N, et. al.	Evaluation for local failure by ^{18}F-FDG PET/CT in comparison with CT findings after stereotactic body radiotherapy (SBRT) for localized non-small-cell lung cancer.	Lung Cancer	79(3)	248-53	2013
Suzuki C, Blomqvist L, Hatschek T, Carlsson L, Fujii H, et. al.	Impact of the first tumor response at eight weeks on overall survival in metastatic breast cancer patients treated with first-line combination chemotherapy.	Med Oncol	30(1)	415	2013
H. Kuno, H. Onaya, S. Fujii, H. Ojiri, M. Satake, et. al.	Primary staging of laryngeal and hypopharyngeal cancer: CT, MR imaging and dual-energy CT.	European Journal of Radiology	83(1)	e23-e35	2014

M. Ikeda, S. Mitsunaga, S. Shimizu, M.Satake, et. al.	Efficacy of sorafenib in patients with hepatocellular carcinoma refractory to transcatheter arterial chemoembolization.	J Gastroenterol	49	932-940	2014
T. Ishihara, T. Kobayashi, N. Ikeno, M. Satake, et. al.	Evaluation of a Near-Infrared-Type Contrast Medium Extravasation Detection System Using a Swine Model.	J Comput Assist Tomogr	38(2)	285-292	2014
M. Sugimoto, S. Takahashi, T. Kobayashi, M. Satake, et. al.	Pancreatic perfusion data and post-pancreaticoduodenectomy outcomes.	Journal of Surgical Research	192(2)	441-9	2015
S. Murata, S. Onozawa, T. Mine, M. Satake, et. al.	Retrograde-outflow percutaneous isolated hepatic perfusion using cisplatin: A pilot study on pharmacokinetics and feasibility.	Eur Radiol	In Press	DOI 10.1007/s00330-014-3558-2	2015
Ahmed S. Maklad, M.Matsuhiro, H.Suzuki, M.Satake, et. al.	Blood vessel-based liver segmentation using the portal phase of an abdominal CT dataset.	Medical Physics	40(11)	113501-1-17	2013
M.Ikeda, T.Okusaka, J.Furuse, M.Satake, et. al.	A multi-institutional phase II trial of hepatic arterial infusion chemotherapy with cisplatin for advanced hepatocellular carcinoma with portal vein tumor thrombosis.	Cancer Chemother Pharmacol	72	463-470	2013
M.Ikeda, S.Mitsunaga, S.Shimizu, M.Satake, et. al.	Efficacy of sorafenib in patients with hepatocellular carcinoma refractory to transcatheter arterial chemoembolization.	J Gastroenterol	49(5)	932-40	2013
H.Kunoa, H.Onaya, S.Fujii, M.Satake, et. al.	Primary staging of laryngeal and hypopharyngeal cancer:CT, MR imaging and dual-energy CT.	European Journal of Radiology	83	e23–e35	2014

Y Akashi, T Oda, Y Ohara1, R Miyamoto, M Satake, et. al.	Anticancer effects of gemcitabine are enhanced by co-administered iRGD peptide in murine pancreatic cancer models that overexpressed neuropilin-1.	Br J CANCER	110(6)	1481-7	2014
Kuno H, Onaya H, Iwata R, Kobayashi T, Satake M, et. al.	Evaluation of cartilage invasion by laryngeal and hypopharyngeal squamous cell carcinoma with dual-energy CT[1].	Radiology	265(2)	488-96	2012
Kojima M, Sudo H, Kawauchi J, Takizawa S, et. al.	MicroRNA Markers for the Diagnosis of Pancreatic and Biliary-Tract Cancers.	PLoS One	10	e0118220	2015
Yokota M, Kojima M, Higuchi Y, Nishizawa Y, et. al.	Spread of tumor microenvironment contributes to colonic obstruction through subperitoneal fibroblast activation in colon cancer.	Cancer Sci	In press.	doi:10.1111/cas.12615.	2015
Ueno H, Shirouzu K, Shimazaki H, Kawachi H, Kojima M, et. al.	Histogenesis and prognostic value of myenteric spread in colorectal cancer: a Japanese multi-institutional study.	J Gastroenterol.	49(3)	400-7	2014
Yamada E, Ishii G, Aramaki N, Aokage K, Kojima M, et. al.	Tumor-size-based morphological features of metastatic lymph node tumors from primary lung adenocarcinoma.	Pathol Int.	64(12)	591-600	2014
Saito N, Ito M, Kobayashi A, Kojima M, et. al.	Long-term outcomes after intersphincteric resection for low-lying rectal cancer.	Ann Surg Oncol	21(11)	3608-15	2014
Kaneko K, Yamaguchi H, Saito T, Kojima M, et. al.	Hypoxia imaging endoscopy equipped with laser light source from preclinical live animal study to first-in-human subject research.	PLoS One	9(6)	e99055	2014

Yokota M, Kojima M, Nomura S, Nishizawa Y, et. al.	Clinical impact of elastic laminal invasion in colon cancer: elastic laminal invasion-positive stage II colon cancer is a high-risk equivalent to stage III.	Dis Colon Rectum	57(7)	830-8.	2014
Sato M, Kojima M, Nagatsuma AK, Nakamura, et. al.	Optimal fixation for total preanalytic phase evaluation in pathology laboratories. A comprehensive study including immunohistochemistry, DNA, and mRNA assays.	Pathol Int.	64(5)	209-16	2014
Sugimoto M, Mitsunaga S, Yoshikawa K, Kojima M, et. al.	Prognostic impact of M2 macrophages at neural invasion in patients with invasive ductal carcinoma of the pancreas.	Eur J Cancer.	50(11)	1900-8	2014
Sugimoto M, Takahashi S, Kojima M, Gotohda N, et. al.	What is the nature of pancreatic consistency? Assessment of the elastic modulus of the pancreas and comparison with tactile sensation, histology, and occurrence of postoperative pancreatic fistula after pancreaticoduodenectomy.	Surgery	156(5)	1204-1117	2014
Kojima M, et. al.	Human subperitoneal fibroblast and cancer cell interaction creates microenvironment that enhances tumor progression and metastasis.	PLoS One	9(2)	e88018	2014
Kojima M, et. al.	Pathological diagnostic criterion of blood and lymphatic vessel invasion in colorectal cancer: a framework for developing an objective pathological diagnostic system using the Delphi method, from the Pathology Working Group of the Japanese Society for Cancer of the Colon and Rectum.	Journal of Clinical Pathology	66(7)	551-558	2013

Kojima M, et al.	Practical utility and objectivity: does evaluation of peritoneal elastic laminal invasion in colorectal cancer overcome these contrary problems?	American Journal of Surgical Pathology	38(1)	144-145	2014
Aizawa M, Kojima M, Gotohda N, Fujii S, et. al.	Geminin expression in pancreatic neuroendocrine tumors: possible new marker of malignancy.	Pancreas	41(4)	512-7	2012
Kawamoto Y, Tsuchihara K, Yoshino T, Ogasawara N, Kojima M, et. al.	KRAS mutations in primary tumours and post-FOLFOX metastatic lesions in cases of colorectal cancer.	Br J Cancer	107(2)	340-4	2012
Hirayama S, Ishii G, Nagai K, Ono S, Kojima M, et. al.	Prognostic impact of CD204-positive macrophages in lung squamous cell carcinoma: possible contribution of Cd204-positive macrophages to the tumor-promoting microenvironment.	J Thorac Oncol	7(12)	1790-7	2012
Makinoshima H, Ishii G, Kojima M, Fujii S, et. al.	PTPRZ1 regulates calmodulin phosphorylation and tumor progression in small-cell lung carcinoma.	BMC Cancer	12	537	2012
Kojima M, Yokota M, Saito N, Nomura S, et. al.	Elastic laminal invasion in colon cancer: diagnostic utility and histological features.	Front Oncol	2	179	2012
Sugimoto M, Gotohda N, Kato Y, Takahashi S, Kojima M, et. al.	Pancreatic resection for metastatic melanoma originating from the Nasal Cavity: A Case Report and Literature Review.	Anticancer Res	33(2)	567-73	2013

研究成果の刊行に関する一覧表

書籍　（日本語）

著者氏名	論文タイトル名	書籍全体の編集者名	書　籍　名	出版社名	出版地	出版年	ページ
小嶋基寛	腫瘍類似病変	青笹克之	癌診療指針のための病理診断プラクティス　肝・胆・膵腫瘍	中山書店	東京	2014	287-293
柴　知史、奥坂拓志	膵がん　2．各論	石岡千加史、井上　忠夫	エビデンスに基づいたがん薬物療法エキスパートマニュアル	総合医学社	東京	2012	125-30
上野　秀樹、奥坂拓志	膵癌	泉　孝英	癌診療の現状.　今日の診療のためにガイドライン外来診療2013	日経メディカル開発	東京	2013	572-73
土原一哉 松島洸達 三牧幸代	全エクソンリシークエンシング	影山博之	次世代シークエンサー：目的別アドバンストメソッド	秀潤社	東京	2012	56-63

雑誌　（日本語）

発表者氏名	論文タイトル名	発表誌名	巻号	ページ	出版年
池田公史、江角浩安	何故，牛蒡子か？	胆と膵	36	105-8	2015
佐々木満仁，上野秀樹，林秀幸，他	膵がんに対する術後補助療法のエビデンスと今後の展望	腫瘍内科	12	259-65	2013
森実千種，奥坂拓志，上野秀樹，他	【外科医が知っておくべき癌治療の薬物療法】抗癌薬各論 胆管癌・膵癌の薬物療法　切除不能・再発癌	外科	75	1369-74	2013

林秀幸，上野秀樹，柴知史	【膵・胆道癌薬物療法:臨床試験を読む!-最新の動向と実地診療へのインパクト-】 局所進行または転移性膵癌に対するGEM+S-1併用療法，S-1単剤療法，またはGEM単剤療法のランダム化第Ⅲ相試験 GEST試験	胆と膵	34	601-06	2013
奥坂拓志	膵がん．早期発見・早期治療のためのがん部位別基礎講座	ヘルスアンドライフ 2月号	第3274号		2012
奥坂拓志、加藤弥菜、荒井保明、上嶋一臣	座談会　肝癌薬物治療のこれから -分子標的治療と経動脈治療-	The Liver Cancer Journal	4(2)	17-25	2012
上野秀樹、奥坂拓志	4.内科治療の進歩、I.膵癌．特集 膵腫瘍：診断と治療の進歩	日本内科学会雑誌	101(1)	29-36	2012
上野秀樹、奥坂拓志	膵癌の化学療法・化学放射線療法．　特集　膵癌診断の最新トピックス	癌と化学療法	39(3)	357-63	2012
坂本康成、上野秀樹、奥坂拓志	膵胆道癌化学療法の最前線．胆・膵疾患診療の最前線・治療/最新の治療戦略とその成果 -病診連携のために-	Medical Practice	29(1)	140-4	2012
池田公史、奥坂拓志	肝癌	薬局	63(4)増刊号	1380-5	2012
池田公史、光永修一、清水　怜、奥坂拓志、他	進行肝細胞癌に対するソラフェニブの現状と今後の展望．進行肝癌治療の現状と今後	日本消化器病学会雑誌	109(8)	1346-54	2012
多田稔、奥坂拓志、古瀬純司、森田智志	【座談会】膵癌治療の新展開；タルセバ・ジェムザール・TS-1	肝胆膵	64(2)	269-86	2012
曽根美雪、荒井保明、奥坂拓志、他	医師主導の多施設共同臨床試験におけるUMINインターネット症例登録センター(UMIN-INDICE)の活用：日本腫瘍IVR研究グループ(Japan Interventional Radiology in Oncology Study Group: JIVROSG)での評価	がんと化学療法	39(4)	619-23	2012

奥坂拓志	標準治療　選択肢が増え二次治療も可能になった化学療法.　特集　膵臓がん　-標準治療と先進治療-	今日の診療のために　ガイドライン外来診療2013	8	14-8	2013
森実千種、奥坂拓志、池田公史	膵消化管神経内分泌腫瘍の内科治療-分子標的薬.　特集：神経内分泌腫瘍を知り尽くす	Mebio	30(4)	88-94	2013
林　秀幸、森実千種、坂本康成、奥坂拓志、他	神経内分泌新生物の化学療法・分子標的治療薬.　特集　消化器神経内分泌腫	臨牀消化器内科	28(1)	113-20	2013
柴　知史、森実千種、林　秀幸、奥坂拓志、他	消化器神経内分泌腫瘍に対する全身化学療法.　特集 消化器癌化学療法-新たなエビデンスを求めて	臨床消化器内科	28(3)	349-56	2013
藤井博史	III 分子イメージングの臨床への展開 2. がんの分子イメージングの現状と展望	Innervision	29 (7)	63-66	2014
梅田泉、木村禎亮、藤井博史	ニトロイミダゾール類とは異なる集積機序をもつ^{99m}Tc標識低酸素イメージングプローブの開発	JSMI report	8 (1)	66-69	2014
梅田泉、藤井博史	臨床応用を目指した分子イメージング研究の現状と今後の展望	日本耳鼻咽喉科学会会報	116 (8)	933-940	2013
久野博文、女屋博昭、佐竹光夫	Centificate of Merit 受賞報告 Imaging of Oropharyngeal Cancer: How Can the Radiologist Help with Treatment Planning?	INNERVISION	28(2)	66	2013
佐藤正明、小嶋基寛、永妻晶子、他	パラフィンブロックの長期保存と採取試料の固定までの時間が与えるKi-67免疫染色，DNAとRNAへの影響	診断病理	32(1)	12-17	2015

小嶋基寛、 落合淳志	大腸癌の最新治療-治癒に向けた最先端研究- 大腸癌の浸潤・転移機構	日本臨牀	72(1)	2-6	2014
小嶋基寛	脈管侵襲の評価法と分類，どうあるべきか	大腸癌 FRONTIER	5	243	2012

厚生労働科学研究費補助金

革新的がん医療実用化研究事業

「我が国で新しく発明された概念に基づく抗がん剤アルクチゲニン臨床第Ⅱ相試験による膵がん克服」に関する研究

平成24年度～平成26年度　総合研究報告書

研究代表者　　江角　浩安

平成27（2015）年　5月

平成24年度

研究成果の刊行物・別刷

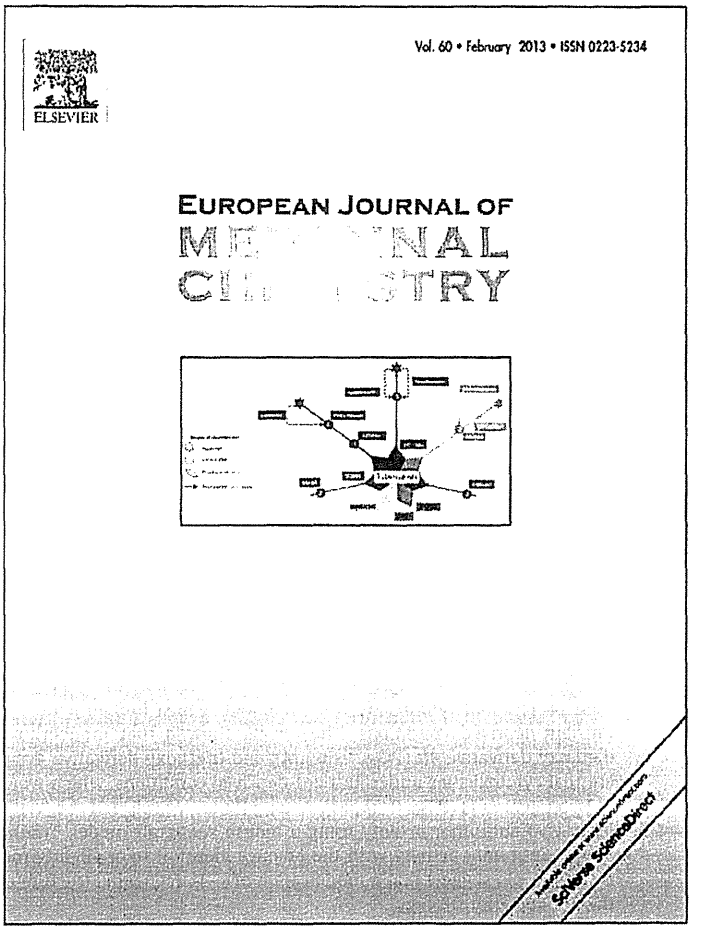

European Journal of Medicinal Chemistry 60 (2013) 76–88

Contents lists available at SciVerse ScienceDirect

European Journal of Medicinal Chemistry

journal homepage: http://www.elsevier.com/locate/ejmech

Original article

Synthesis and antitumor evaluation of arctigenin derivatives based on antiausterity strategy

Naoki Kudou [a], Akira Taniguchi [b], Kenji Sugimoto [a], Yuji Matsuya [a], Masashi Kawasaki [c], Naoki Toyooka [b,d,*], Chika Miyoshi [e], Suresh Awale [f], Dya Fita Dibwe [g], Hiroyasu Esumi [e], Shigetoshi Kadota [g], Yasuhiro Tezuka [g,**]

[a] Graduate School of Medicine and Pharmaceutical Sciences, University of Toyama, 2630 Sugitani, Toyama, 930-0194, Japan
[b] Graduate School of Science and Technology for Research, University of Toyama, 3190 Gofuku, Toyama 930-8555, Japan
[c] Department of Liberal Arts and Sciences, Faculty of Engineering, Toyama Prefectural University, 5180 Kurokawa, Kosugi-Machi, Toyama 939-0398, Japan
[d] Graduate School of Innovative Life Science, University of Toyama, 3190 Gofuku, Toyama 930-8555, Japan
[e] Cancer Physiology Project, Research Center for Innovative Oncology, National Cancer Center Hospital East, Chiba, Japan
[f] Frontier Research Core for Life Sciences, University of Toyama, 2630 Sugitani, Toyama 930-0194, Japan
[g] Institute of Natural Medicine, University of Toyama, 2630 Sugitani, Toyama 930-0194, Japan

ARTICLE INFO

Article history:
Received 24 July 2012
Received in revised form
14 September 2012
Accepted 21 November 2012
Available online 28 November 2012

Keywords:
(−)-Arctigenin derivatives
Antiausteric activity
Synthesis
Pancreatic cancer

ABSTRACT

A series of new (−)-arctigenin derivatives with variably modified *O*-alkyl groups were synthesized and their preferential cytotoxicity was evaluated against human pancreatic cancer cell line PANC-1 under nutrient-deprived conditions. The results showed that monoethoxy derivative **4l** (PC_{50}, 0.49 μM), diethoxy derivative **4h** (PC_{50}, 0.66 μM), and triethoxy derivative **4m** (PC_{50}, 0.78 μM) showed the preferential cytotoxicities under nutrient-deprived conditions, which were identical to or more potent than (−)-arctigenin (**1**) (PC_{50}, 0.80 μM). Among them, we selected the triethoxy derivative **4m** and examined its *in vivo* antitumor activity using a mouse xenograft model. Triethoxy derivative **4m** exhibited also *in vivo* antitumor activity with the potency identical to or slightly more than (−)-arctigenin (**1**). These results would suggest that a modification of (−)-arctigenin structure could lead to a new drug based on the antiausterity strategy.

1. Introduction

Pancreatic cancer is the most aggressive cancer of all and has an exceptionally high global mortality rate, with an estimated 267,000 deaths worldwide in 2008. It ranks 8th or 9th as the most frequent cause of cancer death worldwide and is the 4th or 5th most frequent cause of cancer death in most developed countries, including the United States, Europe, and Japan [1]. Moreover, it has been estimated that the number of deaths from pancreatic cancer will reach 484,000 by 2030 [1]. Pancreatic cancer rapidly metastases and lead the patients to die in a short period of the diagnosis. Thus, the 5-year survival rate of the patients with the pancreatic cancer is the lowest among several cancers [2,3]. Though surgery is the only treatment method that offers any prospect of potential cure, chemotherapy with 5-fluorouracil and gemcitabine is also used for palliative therapy of advanced pancreatic cancer. However pancreatic cancer is largely resistant to most known chemotherapeutic agents including 5-fluorouracil and gemcitabine [4]. Therefore effective chemotherapeutic agents that target pancreatic cancer are urgently needed.

Tumor cells, in general, proliferate very fast, and the demand for essential nutrients, oxygen, *etc.* is always high. The immediate environment of cancers increasing in size, however, often becomes heterogeneous and some regions of large cancers often possess microenvironmental niches, which exhibit a significant gradient of critical metabolites including oxygen, glucose, other nutrients, and growth factors [5]. Thus, many cancer cells get the critical metabolites by randomly recruiting new blood vessels, a phenomenon commonly known as angiogenesis, to survive under such severe conditions. However, human pancreatic cancer survives with an extremely poor blood supply and becomes more malignant [6]. The method by which pancreatic cancer survives is by getting a remarkable tolerance to extreme nutrient starvation [7]. Therefore, it has been hypothesized that eliminating the tolerance of cancer cells to nutrition starvation

* Corresponding author. Graduate School of Science and Technology for Research, University of Toyama, 3190 Gofuku, Toyama 930-8555, Japan. Tel.: +81 76 445 6859.
** Corresponding author. Tel.: +81 76 434 7627; fax: +81 76 434 5059.
E-mail addresses: toyooka@eng.u-toyama.ac.jp (N. Toyooka), tezuka@inm.u-toyama.ac.jp (Y. Tezuka).

0223-5234/$ – see front matter © 2012 Elsevier Masson SAS. All rights reserved.
http://dx.doi.org/10.1016/j.ejmech.2012.11.031

may allow a novel biochemical approach known as "anti-austerity" for cancer therapy [8].

In this regard, we screened 500 medicinal plants used in Kampo medicine to identify agents that preferentially reduce the survival of nutrient-deprived human pancreatic cancer PANC-1 cells. The screen led to the isolation of (−)-arctigenin (**1**) as the active principle of *Arctium lappa* [9]. In addition to pancreatic cancer, arctigenin has been reported to inhibit lung, skin, and stomach cancers [10]. Thus, we started the synthetic work of arctigenin derivatives to obtain more effective drugs against pancreatic cancer. In *A. lappa*, (−)-arctigenin is mainly contained as its glucoside, arctiin, and after consumption arctiin was reported to be deglucosidated to (−)-arctigenin (**1**), followed by demethylation and dehydroxylation by intestinal bacteria to metabolites **I**–**V** [11]. As reported previously, (−)-arctigenin showed potent preferential cytotoxicity, whereas its glucoside, arctiin, showed no cytotoxicity [9]. In our preliminary examination, moreover, metabolites **I** and **V** (Fig. 1) showed weaker activity. These facts should suggest that the 4′-hydroxyl group should be important for the preferential cytotoxicity and that (−)-arctigenin is deactivated through the demethylation/demethoxylation. In addition, the enantiomer of (−)-arctigenin (**1**), (+)-arctigenin (Fig. 1), showed very weak preferential cytotoxicity, indicating the importance of the 2*R*,3*R* absolute stereochemistry of (−)-form. Thus, with an intention to improve the metabolism stability, we have synthesized 15 arctigenin derivatives **4a**–**o** with different alkoxy substituent and the 2*R*,3*R*-configuration, and the *in vitro* preferential cytotoxicity of them was characterized under nutrient-deprived conditions. Then, the triethoxy derivative **4m**, exhibiting the *in vitro* activity identical to **1** and having no methoxy group which may be metabolized, was selected and further evaluated the effect against tumor cell growth *in vivo* in a cancer xenograft mouse model.

2. Results and discussion

2.1. Chemistry

First we planned the synthesis of derivatives on the 3′ position of (−)-arctigenin. For this purpose, (−)-arctigenin (**1**) was converted to the diol **2** [12], which was transformed into 6 derivatives **4a**–**f** via selective protection of **2**, alkylation of **3**, followed by deprotection of the benzyl group (Scheme 1).

Next we planned the efficient and flexible synthesis of a variety of derivatives on the 3′, 3″, and 4″ positions of (−)-arctigenin.

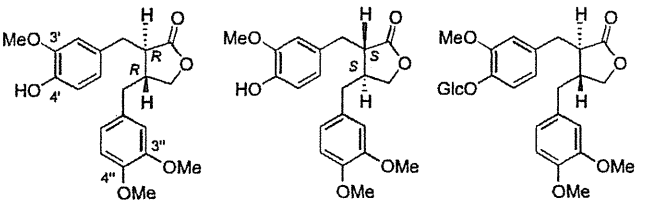

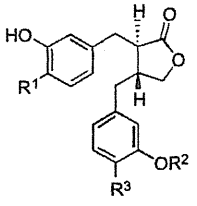

	R1	R2	R3
I	OH	Me	OMe
II	H	Me	OMe
III	H	H	OMe
IV	H	H	OH
V	H	H	H

Fig. 1. Structures of (−)-arctigenin (**1**) and its analogs.

3,4-Dihydroxybenzaldehyde was converted to the alcohol **7** via known benzyl ether **5** [13] and aldehyde **6** [14]. Mono-alkylation of diethyl malonate with the mesylate of **7** afforded the ester **8**. Reduction of **8** and lipase-mediated transesterification of the resulting diol provided the mono-acetate (+)-**9**. The enantiomeric excess of (+)-**9** was determined to be 98% ee by the HPLC analysis using the chiral column (Chiralcel OJ). The absolute stereochemistry of (+)-**9** was determined by the comparison of the optical rotation with known lactone **13a**, prepared from (+)-**9** via mesylate **10**, benzyl ether **11**, and lactone **12a** as shown in Scheme 2. Other lactones **13b**–**f** were also prepared from (+)-**9**, and these lactones **13b**–**f** were alkylated on the α-position with several alkyl halides to afford the di-substituted lactones **14a**–**i**. Finally deprotection of the benzyl group furnished the desired derivatives **4g**–**o**.

From the comparison of the *in vitro* activity of the synthesized derivatives **4a**–**o** against the human pancreatic cancer cell line PANC-1, the triethoxy derivative **4m** was chosen as the potent candidate for the *in vivo* experiment. As the more effective synthesis of **4m**, we investigated the modified synthesis of the lactone **13d**. 3,4-Dihydroxybenzaldehyde was converted to the ester **17** via known aldehyde **15** [15] and alcohol **16** [16] as the same procedure for the synthesis of **8**. After reduction of **17**, lipase-mediated transesterification of the resulting diol afforded the mono-acetate **18**, whose enantiomeric excess was determined to be 98% ee again by the Mosher method. The mono-acetate **18** was then transformed into the lactone **13d** via mesylate **19** (Scheme 3).

2.2. In vitro preferential cytotoxicity of arctigenin derivatives

All of the (−)-arctigenin derivatives **4a**–**o** were evaluated for their *in vitro* preferential cytotoxic activity against human pancreatic cancer PANC-1 cells in nutrient-deprived medium (NDM). The PANC-1 cell line is highly resistant to nutrient starvation, and can survive in NDM even after 48 h of starvation [6,7,8]. However, this tolerance to nutrient starvation was remarkably eliminated by the tested compounds in a concentration-dependent manner. The tested compounds exhibited different potency of toxicity (Fig. 2) and their preferential cytotoxicities are obtained as the 50% cytotoxic concentration in NDM (PC_{50} value) (Table 1). Among the (−)-arctigenin derivatives **4a**–**o**, monoethoxy derivative **4i** showed the most potent preferential cytotoxicity (PC_{50}, 0.49 μM), followed by diethoxy derivative **4h** (PC_{50}, 0.66 μM) and triethoxy derivative **4m** (PC_{50}, 0.78 μM), which were identical to or more potent than (−)-arctigenin (**1**) (PC_{50}, 0.80 μM).

On the relationship between the substituents and the preferential activity, the 3′ position seems to favor smaller substituent since the PC_{50} values of **1** and **4a**–**d** increase in the order: **1** (MeO) < **4a** (EtO) = **4b** (*n*-PrO) < **4c** (*i*-PrO) < **4d** (*n*-BuO). This would suggest the importance of the 4′-hydroxy group for the preferential activity. On the other hand, there is not clear relationship on the substituents at the 3″ and 4″ positions, although smaller substituents seems to be favor.

The order of *in vitro* preferential cytotoxicity (PC_{50}) was **4i** > **4h** > **4m**. Whereas **4h** and **4i** have the methoxy groups which was reported to be demethylated and then deoxygenated by intestinal bacteria and/or hepatic enzyme [11]. Thus, we selected the triethoxy derivative **4m** to pursue a further examination, from a viewpoint of metabolism stability.

2.3. In vivo antitumor activity of triethoxy derivative 4m

The triethoxy derivative **4m** showed the *in vitro* preferential cytotoxicity also against human pancreatic cancer cell line CAPAN-1 under glucose deficient conditions with a intensity similar to (−)-arctigenin (**1**) (Fig. 3). We used PANC-1 cell line for *in vitro*

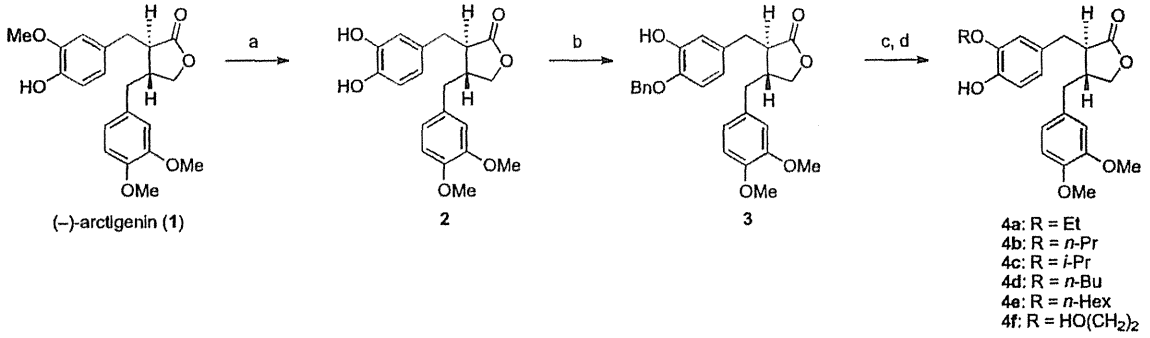

Scheme 1. Reagents and conditions: a: $AlCl_3$, pyridine, CH_2Cl_2, reflux (quant.); b: BnBr, K_2CO_3, KI, acetone, reflux (63%); c: *RI* or RBr, K_2CO_3, acetone, reflux for **4a–e** or 2-benzyloxyethanol, Ph_3P, DEAD, CH_2Cl_2, rt for **4f**; d: H_2, $Pd(OH)_2$, MeOH, rt.

study because of its ready growth [17], while mouse xenograft model can be prepared with CAPAN-1 cell line more easily than with PANC-1 cell line [18]. Thus, we used mouse xenograft model with CAPAN-1 cell line for comparing the *in vivo* effect of triethoxy derivative **4m** with (−)-arctigenin (**1**).

Mice were inoculated with 5×10^6 CAPAN-1 cells s.c. on the back and then administered triethoxy derivative **4m**, (−)-arctigenin (**1**), or vehicle, as described in Experimental. The body weight of the animals was monitored weekly (Fig. 4A) and no significant body weight loss was recognized in the treated group versus the vehicle control group at any time during the experimental period. This fact, together with the behavior of the treated animals, indicated that the tested compounds might have no toxicity at the dose used. The treatment was initiated from the 15th day by i.p. injection of the drug at the dose of 50 μg/mouse/d on 6 days of the week (or vehicle in the control group) until the 28th day. The tumor size was measured weekly. As is evident from the tumor growth curve shown in Fig. 4B, the tumor volume increased steadily in the control group, whereas the increase was significantly less prominent in the groups treated by triethoxy derivative **4m** or (−)-arctigenin (**1**). There was a significant difference in the tumor size at the day 21 between the groups treated by triethoxy derivative **4m** or (−)-arctigenin (**1**) and the control group ($P < 0.05$). Similarly, the mean wet weight and the size of the tumor were higher in the

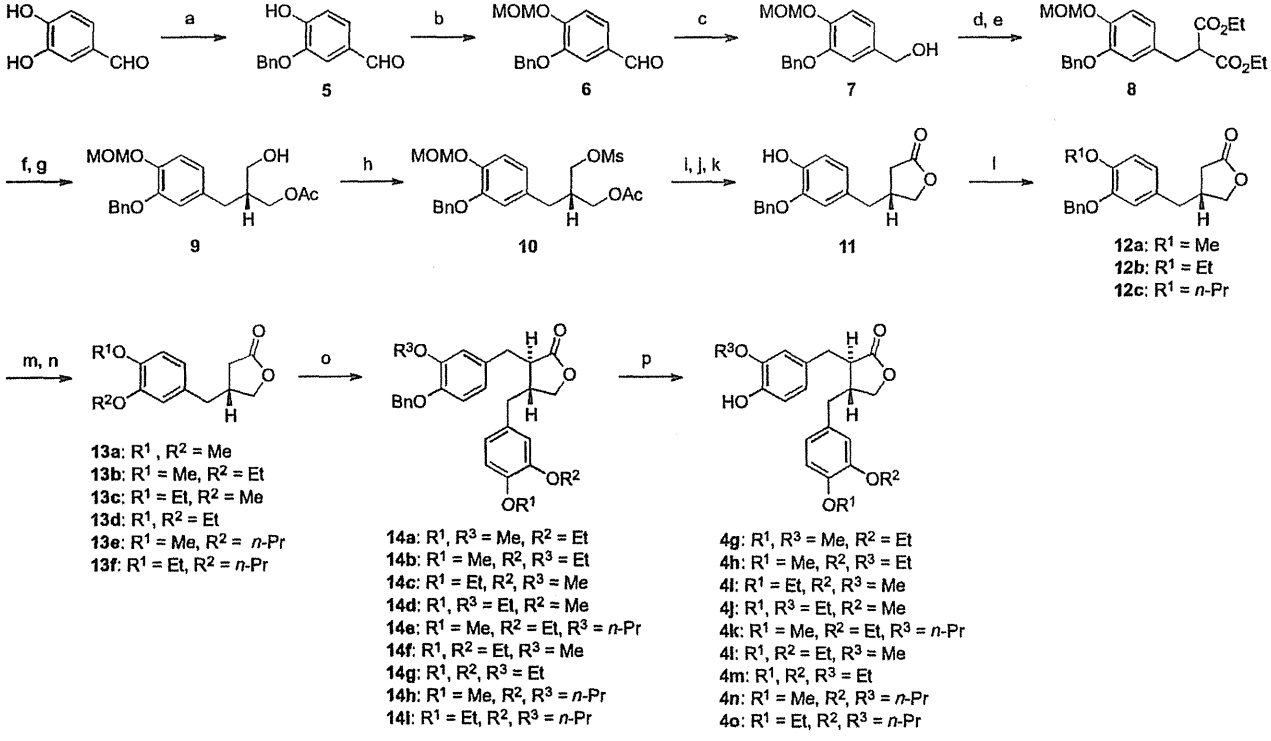

Scheme 2. Reagents and conditions: a: BnBr, K_2CO_3, KI, acetone, reflux (64%); b: MOMCl, DIPEA, CH_2Cl_2, rt (quant.); c: $NaBH_4$, MeOH, rt (95%); d: MsCl, Et_3N, CH_2Cl_2, rt; e: diethyl malonate NaH, DMF, rt (72% in 2 steps); f: $LiAlH_4$, THF, reflux; g: lipase-PS (Amano), vinyl acetate, *i*-Pr_2O–THF rt (80% in 2 steps, 98% ee); h: MsCl, Et_3N, CH_2Cl_2, rt; i: KCN, DMSO, 90 °C; j: LiOH, THF–H_2O, rt; k: 10% NaOH (aq), reflux, then 10% HCl (aq)–THF, rt (73% in 4 steps); l: MeI or EtI or *n*-PrBr, K_2CO_3, acetone, reflux (88% for **12a**, 86% for **12b**, 87% for **12c**); m: H_2, $Pd(OH)_2$, MeOH; *n*: MeI or EtI, K_2CO_3, acetone, reflux (55% in 2 steps for **13a**, 55% in 2 steps for **13b**, 55% in 2 steps for **13c**, 47% in 2 steps for **13d**, 80% in 2 steps for **13e**, 77% in 2 steps for **13f**); o: LiHMDS, substituted BnBr, HMPA, THF, −78 °C to rt (44% for **14a**, 59% for **14b**, 43% for **14c**, 53% for **14d**, 40% for **14e**; 48% for **14f**; 56% for **14g**, 49% for **14h**; 33% for **14i**); p: H_2, $Pd(OH)_2$, MeOH (89% for **4g**, 63% for **4h**, 57% for **4i**, 63% for **4j**, 56% for **4k**, 81% for **4l**, 66% for **4m**, 46% for **4n**, 63% for **4o**).

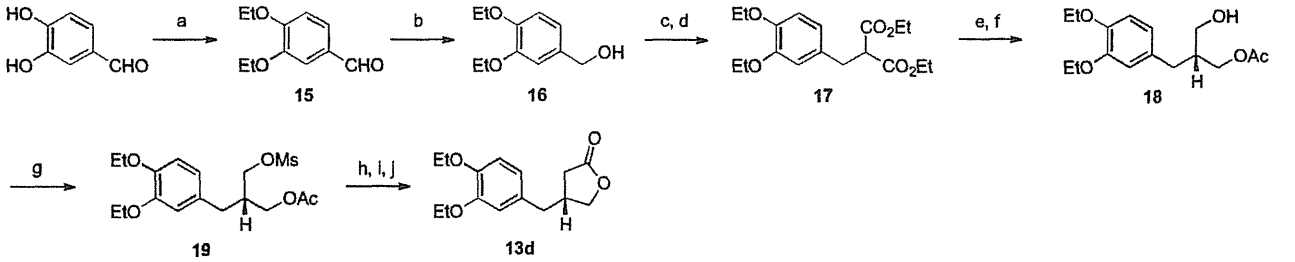

Scheme 3. Reagents and conditions: a: EtI, K_2CO_3, acetone, reflux (92%); b: $NaBH_4$, MeOH, rt (74%); c: MsCl, Et_3N, CH_2Cl_2, rt; d: diethyl malonate NaH, DMF, rt (87% in 2 steps); e: $LiAlH_4$, THF, reflux; f: lipase-PS (Amano), vinyl acetate, *i*-Pr_2O–THF rt (53% in 2 steps, 98% ee); g: MsCl, Et_3N, CH_2Cl_2, rt (79%); h: KCN, DMSO, 90 °C; i: LiOH, THF–H_2O, rt; j: 10% NaOH (aq), reflux, then 10% HCl (aq)-THF, rt (60% in 3 steps).

control group than the groups treated by triethoxy derivative **4m** or (−)-arctigenin (**1**) (Fig. 4C–F). These data indicate that triethoxy derivative **4m** also exerted antitumor activity *in vivo* with the potency identical to or slightly more than (−)-arctigenin (**1**).

3. Conclusion

In summary, a series of new (−)-arctigenin derivatives modified on *O*-alkyl groups were synthesized and their preferential cytotoxicity was evaluated against human pancreatic cancer cell line PANC-1 under nutrient-deprived conditions. The results showed that monoethoxy derivative **4i** (PC_{50}, 0.49 μM), diethoxy derivative **4h** (PC_{50}, 0.66 μM), and triethoxy derivative **4m** (PC_{50}, 0.78 μM) showed the preferential cytotoxicities under nutrient-deprived conditions, which were identical to or more potent than (−)-arctigenin (**1**) (PC_{50}, 0.80 μM). Among them, we selected the triethoxy derivative **4m** and examined *in vivo* antitumor activity with mouse xenograft model. Triethoxy derivative **4m** exhibited also *in vivo* antitumor activity with the potency identical to (−)-arctigenin (**1**). These results would suggest that a modification of (−)-arctigenin structure could lead to a new drug based on the antiausterity strategy.

4. Experimental

4.1. Chemistry

4.1.1. General conditions

Chemicals were purchased from Sigma–Aldrich, Merck, Nakalai Tesque, Wako Pure Chemicals, and Kanto Chemicals, and used without further purification. Column chromatography was done on Cica silica gel 60N (spherical, neutral; particle size, 40–50 μm, Kanto Chemical Co., Inc., Tokyo, Japan), while thin-layer chromatography (TLC) was performed on Merck silica gel $60F_{254}$ plates (Merck KGaA, Darmstadt, Germany). Melting points were taken on a Yanaco micromelting point apparatus and are uncorrected. The nuclear magnetic resonance (NMR) spectra were acquired in the specified solvent, in a Varian Gemini 300 spectrometer (300 and 75 MHz for ^1H and ^{13}C, respectively) or Varian UNITY plus 500 spectrometer (500 and 125 MHz for ^1H and ^{13}C, respectively) (Varian Inc., Palo Alto, CA, USA), with tetramethylsilane (TMS) as internal standard. The chemical shifts (δ) are reported in ppm downfield from TMS and coupling constants (J) are expressed in Hertz. Optical rotations were obtained in the specified solvent on a JASCO DIP-1000 digital polarimeter (JASCO Corp., Tokyo, Japan). IR spectra were measured with a JASCO FT/IR-460 Plus spectrophotometer (JASCO Corp.). The low-resolution mass spectra (MS) and high-resolution mass spectra (HRMS) were obtained with a Shimadzu GCMS-QP 500 mass spectrometer (Shimadzu Corp., Kyoto, Japan), JEOL D-200, or JEOL AX505 mass spectrometer (JEOL Ltd., Tokyo, Japan) in the electron impact mode at the ionization potential of 70 eV.

4.1.2. Synthesis of (−)-arctigenin derivatives **4a–4f**

*4.1.2.1. (3R,4R)-3-(4-Benzyloxy-3-hydroxybenzyl)-4-(3,4-dimethoxybenzyl)dihydrofuran-2-one (**3**).* To a stirred solution of (3R,4R)-3-(3,4-dihydroxybenzyl)-4-(3,4-dimethoxybenzyl)dihydrofuran-2-one (**2**) [12] (65.4 mg, 0.18 mmol) in acetone (2 mL) were added K_2CO_3 (37.3 mg, 0.27 mmol), KI (5.97 mg, 0.036 mmol), and BnBr (21.4 μL, 0.18 mmol), and the resulting mixture was refluex for 5 h. After cooling, the reaction mixture was filtered, and the filtrate was evaporated. The residue was chromatographed on silica gel (10 g, hexane:acetone = 4:1) to give **3** (51.2 mg, 63%) as a pale yellow oil: ^1H NMR (300 MHz, $CDCl_3$) δ: 1.60 (1H, br), 2.47–2.63 (4H, m), 2.86–2.98 (2H, m), 3.80 (3H, s), 3.85 (3H, s), 3.80–3.89 (1H, m), 4.09–4.14 (1H, m), 5.13 (2H, s), 6.47–6.80 (6H, m), 7.28–7.44 (5H, m); ^{13}C NMR (75 MHz, $CDCl_3$) δ: 34.59, 38.19, 41.15, 46.53, 55.82, 55.98, 71.08, 71.21, 111.22, 111.72, 112.79, 113.95, 120.43, 121.20, 127.12, 127.69, 128.39, 130.30, 130.73, 136.98, 146.91, 147.67, 148.84, 149.63, 178.46; IR (neat): 1514 (C=C), 1769 (C=O) cm^{-1}; MS (EI) *m/z* 449 (M^+); HRMS (EI): calcd for $C_{27}H_{28}O_6$: 448.1886 (M^+), found: 448.2743; $[\alpha]_D^{26}$ −20.7 (*c* 0.85, $CHCl_3$).

*4.1.2.2. (3R,4R)-4-(3,4-Dimethoxybenzyl)-3-(3-ethoxy-4-hydroxybenzyl)dihydrofuran-2-one (**4a**).* To a stirred solution of **3** (44.7 mg, 0.10 mmol) in acetone (5 mL) were added K_2CO_3 (82.6 mg, 0.60 mmol), EtI (26.5 μL, 0.33 mmol), and the reaction mixture was refluxed for 48 h. After cooling, the reaction mixture was filtered, and the filtrate was evaporated. The residue was dissolved in MeOH (6 mL). To the solution was added 20% $Pd(OH)_2$ (10 mg), and the resulting suspension was stirred under a hydrogen atmosphere at 1 atm for 16 h. The catalyst was removed by filtration and the filtrate was evaporated. The residue was chromatographed on silica gel (7 g, hexane : acetone = 3:1) to give **4a** (13.4 mg, 35% in 2 steps) as a colorless oil: ^1H NMR (300 MHz, $CDCl_3$) δ: 1.41 (3H, t, J = 7.1 Hz), 2.42–2.64 (4H, m), 2.90 (2H, d, J = 5.2 Hz), 3.80 (3H, s), 3.84 (3H, s), 3.80–3.88 (1H, m), 4.02 (2H, q, J = 7.1 Hz), 4.08–4.13 (1H, m), 5.66 (1H, br), 6.46–6.75 (4H, m), 6.81 (1H, d, J = 8.0 Hz); ^{13}C NMR (75 MHz, $CDCl_3$) δ: 14.85, 30.94, 34.48, 38.15, 40.90, 46.58, 55.85, 64.38, 71.24, 111.11, 111.61, 112.29, 113.94, 120.43, 121.83, 129.20, 130.30, 144.47, 145.80, 147.62, 148.81, 178.51; IR (neat): 1516 (C=C), 1766 (C=O), 3446 (OH) cm^{-1}; MS (EI) *m/z* 386 (M^+); HRMS (EI): calcd for $C_{22}H_{26}O_6$: 386.1729 (M^+), found: 386.1724; $[\alpha]_D^{26}$ −20.5 (*c* 0.98, $CHCl_3$).

*4.1.2.3. (3R,4R)-4-(3,4-Dimethoxybenzyl)-3-(4-hydroxy-3-propoxybenzyl)dihydrofuran-2-one (**4b**).* By the procedure similar to synthesis of **4a**, (−)-arctigenin derivative **4b** was prepared from **3** and *n*-PrBr (18% in 2 steps) as a colorless oil: ^1H NMR (300 MHz, $CDCl_3$) δ: 1.04 (3H, t, J = 1.9 Hz), 1.77–1.87 (2H, m), 2.42–2.67 (4H, m), 2.81–3.01 (2H, m), 3.78–3.86 (7H, m), 3.90–4.00 (2H, m), 4.09–4.14 (1H, m), 5.59–5.63 (1H, br), 6.47–6.85 (6H, m); ^{13}C NMR (75 MHz, $CDCl_3$) δ: 10.60, 22.60, 29.34, 31.81, 34.55, 38.22, 41.49, 46.65, 53.80, 55.82, 70.35, 71.29, 111.71, 113.94, 115.27, 120.47, 121.85, 112.34, 129.28,

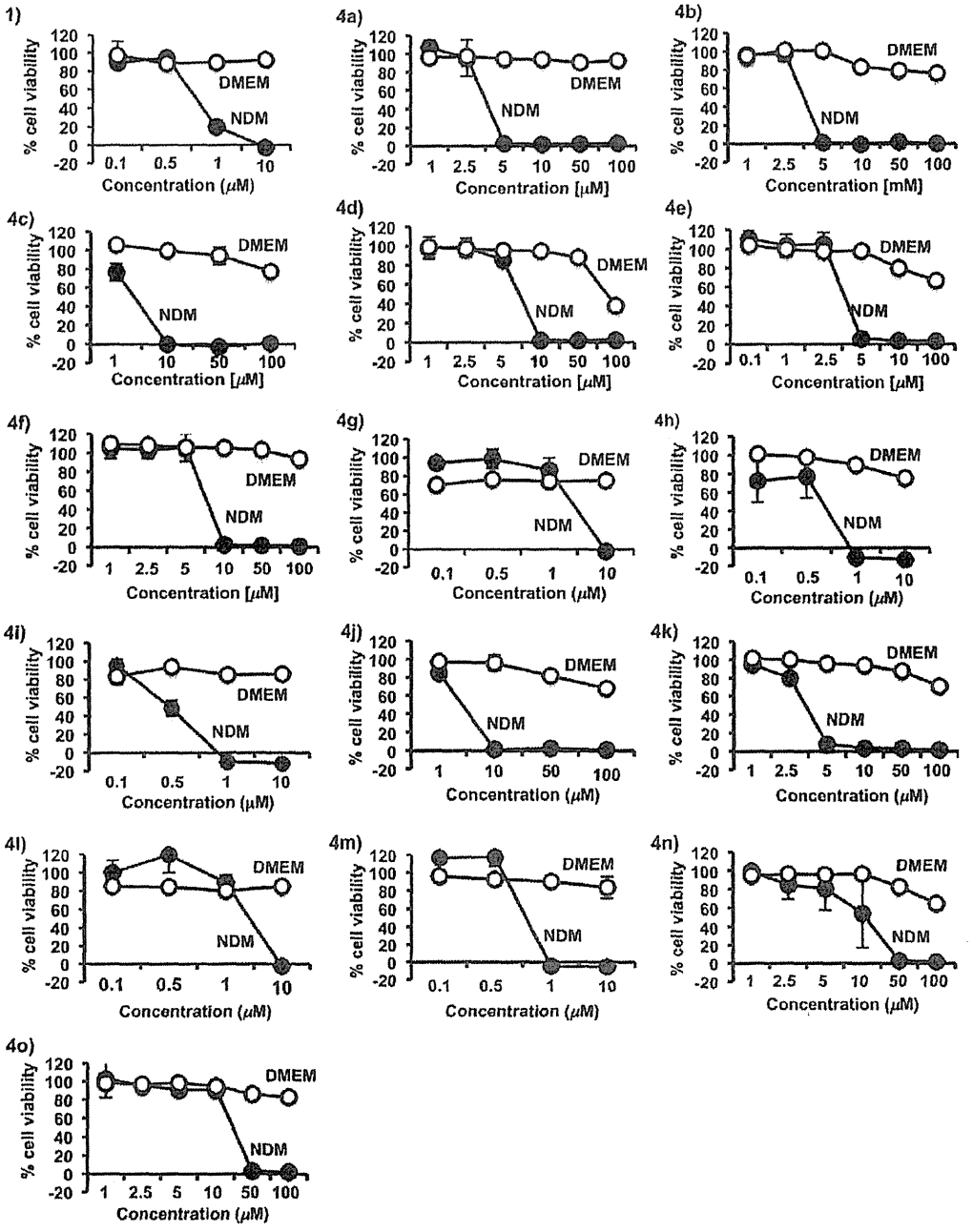

Fig. 2. Effects of (−)-arctigenin derivatives on cell survival in the PANC-1 cell line under nutrient-deprived conditions. Cells were seeded at a density of 2×10^4 per well in 96-well plates and incubated in fresh complete medium for 24 h. The cells were then washed with PBS and the medium was changed to nutrient-deprived medium (NDM, ●) or normal DMEM (○) together containing graded concentrations of (−)-arctigenin derivatives. Points, mean from triplicate experiments. The cell number at the start of the starvation was considered to be 100%. The cell count was measured by the WST-8 cell counting kit method, as described in experimental. The numbers **1** and **4a–o** mean the data of (−)-arctigenin (**1**) and (−)-arctigenin derivatives **4a–o**, respectively.

130.59, 144.52, 147.69, 178.54; IR (neat): 1456 (C=C), 1769 (C=O) cm^{-1}; MS (EI) *m/z* 400 (M^+); HRMS (EI): calcd for $C_{23}H_{28}O_6$: 400.1886 (M^+), found: 400.1893; $[\alpha]_D^{26}$ −15.7 (*c* 1.45, $CHCl_3$).

4.1.2.4. (3R,4R)-4-(3,4-Dimethoxybenzyl)-3-(4-hydroxy-3-i-propoxybenzyl)dihydrofuran-2-one (4c). By the procedure similar to synthesis of **4a**, (−)-arctigenin derivative **4c** was prepared from **3** and *i*-PrI (18% in 2 steps) as a pale yellow oil: ^1H NMR (300 MHz, $CDCl_3$) δ: 1.31–1.35 (6H, m), 1.59 (1H, br), 2.41–2.68 (4H, m), 2.80–3.00 (2H, m), 3.80–3.88 (7H, m), 4.07–4.12 (1H, m), 4.49–4.57 (1H, m), 6.48–6.84 (6H, m); ^{13}C NMR (75 MHz, $CDCl_3$) δ: 22.02, 34.39, 3.12, 41.45, 46.65, 55.81, 71.19, 111.25, 111.68, 113.41, 114.18, 115.49, 120.61, 122.09, 129.26, 130.43, 144.70, 145.48, 146.59, 147.84, 149.02, 178.72; IR (neat): 1716 (C=O), 3629 (OH) cm^{-1}; MS (EI) *m/z* 400 (M^+); HRMS (EI): calcd for $C_{23}H_{28}O_6$: 400.1886 (M^+), found: 400.1926; $[\alpha]_D^{24}$ −37.7 (*c* 0.41, $CHCl_3$).

4.1.2.5. (3R,4R)-4-(3,4-Dimethoxybenzyl)-3-(4-hydroxy-3-butyloxybenzyl)dihydrofuran-2-one (4d). By the procedure similar to synthesis of **4a**, (−)-arctigenin derivative **4d** was prepared from **3**

Table 1
Preferential cytotoxicity of (−)-arctigenin (**1**) and series of new (−)-arctigenin derivatives **4a–4o** against human pancreatic cancer PANC-1 cells in nutrient-deprived medium (NDM).

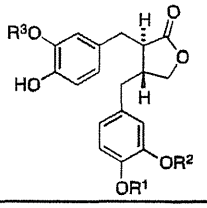

Compound	R^1	R^2	R^3	PC_{50} (μM)	Compound	R^1	R^2	R^3	PC_{50} (μM)
1 (arctigenin)	Me	Me	Me	0.80	**4h**	Me	Et	Et	0.66
4a	Me	Me	Et	3.74	**4i**	Et	Me	Me	0.49
4b	Me	Me	*n*-Pr	3.74	**4j**	Et	Me	Et	4.77
4c	Me	Me	*i*-Pr	4.16	**4k**	Me	Et	*n*-Pr	3.54
4d	Me	Me	*n*-Bu	7.14	**4l**	Et	Et	Me	4.85
4e	Me	Me	*n*-Hex	3.89	**4m**	Et	Et	Et	0.78
4f	Me	Me	$HO(CH_2)_2$	7.70	**4n**	Me	*n*-Pr	*n*-Pr	13.6
4g	Me	Et	Me	4.71	**4o**	Et	*n*-Pr	*n*-Pr	28.6

and *n*-BuBr (25% in 2 steps) as a colorless oil: ^{1}H NMR (300 MHz, $CDCl_3$) δ: 0.98 (3H, t, J = 7.1 Hz), 1.48 (2H, dd, J = 15.1, 7.1 Hz), 1.74–1.83 (2H, m), 2.41–2.66 (4H, m), 2.80–3.02 (2H, m), 3.82 (3H, s), 3.83 (3H, s), 3.85 (1H, m), 3.94–4.03 (2H, m), 4.08–4.14 (1H, m), 5.59 (1H, m), 6.50–6.84 (6H, m); ^{13}C NMR (75 MHz, $CDCl_3$) δ: 13.97, 19.32, 31.31, 55.82, 55.92, 68.60, 68.65, 71.21, 71.27, 111.19, 111.67, 112.32, 113.92, 120.46, 129.29, 130.34, 130.46, 144.52, 144.71, 145.59, 145.96, 147.69, 148.92, 178.53; IR (neat): 1515 (C=C), 1769 (C=O), 3446 (OH) cm^{-1}; MS (EI) *m/z* 414 (M^+); HRMS (EI): calcd for $C_{24}H_{30}O_6$: 414.2042 (M^+), found: 414.2000; $[\alpha]_D^{26}$ −20.2 (*c* 1.15, $CHCl_3$).

4.1.2.6. (3R,4R)-4-(3,4-Dimethoxybenzyl)-3-(3-hexyloxy-4-hydroxybenzyl)dihydrofuran-2-one (4e). By the procedure similar to synthesis of **4a**, (−)-arctigenin derivative **4e** was prepared from **3** and 1-bromohexane (35% in 2 steps) as a pale yellow oil: ^{1}H NMR (300 MHz, $CDCl_3$) δ: 0.90 (3H, t, J = 6.4 Hz), 1.25–1.27 (2H, m), 1.33–1.35 (4H, m), 1.45 (2H, m), 1.75–2.66 (4H, m), 2.81–3.01 (2H, m), 3.82 (3H, s), 3.85 (3H, s), 3.84–3.89 (1H, m), 3.94–4.02 (2H, m), 4.09–4.14 (1H, m), 5.56–5.61 (1H, m), 6.47–6.84 (6H, m); ^{13}C NMR (75 MHz, $CDCl_3$) δ: 14.11, 22.67, 25.78, 29.25, 31.62, 34.56, 38.22, 40.02, 46.65, 55.82, 68.92, 71.21, 111.19, 111.67, 112.32, 113.92, 115.25, 120.56, 121.83, 129.29, 130.43, 130.34, 144.52, 147.67, 148.92, 178.53; IR (neat): 1457 (C=C), 1764 (C=O), 3689 (OH) cm^{-1}; MS (EI) *m/z* 442 (M^+); HRMS (EI): calcd for $C_{26}H_{34}O_6$: 442.2355 (M^+), found: 442.2336; $[\alpha]_D^{26}$ −10.1 (*c* 0.65, $CHCl_3$).

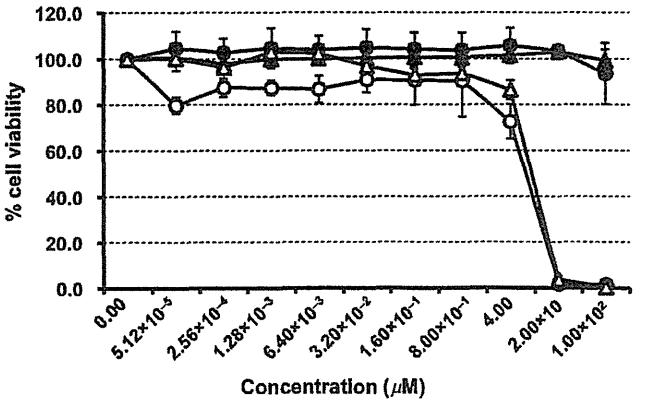

Fig. 3. Effect of triethoxy derivative **4m** and (−)-arctigenin (**1**) on cell survival in the CAPAN-1 cell line under glucose-deprived conditions. ●, (−)-arctigenin (**1**) in normal DMEM; ▲, triethoxy derivative **4m** in normal DMEM; ○, (−)-arctigenin (**1**) in glucose-deprived medium; △, triethoxy derivative **4m** in glucose-deprived medium.

4.1.2.7. (3R,4R)-4-(3,4-Dimethoxybenzyl)-3-[4-hydroxy-3-(2-hydroxyethoxy)benzyl]dihydrofuran-2-one (4f). By the procedure similar to synthesis of **4a**, (−)-arctigenin derivative **4f** was prepared from **3** and 2-benzyloxyethanol (20% in 2 steps) as a colorless oil: ^{1}H NMR (300 MHz, $CDCl_3$) δ: 2.42–2.59 (4H, m), 2.78–2.94 (2H, m), 3.76 (3H, s), 3.83 (3H, s), 3.73–3.80 (1H, m), 3.86–4.07 (6H, m), 4.13–4.16 (1H, m), 6.40–6.75 (4H, m), 6.81 (1H, d, J = 8.0 Hz); ^{13}C NMR (75 MHz, $CDCl_3$) δ: 28.24, 38.22, 40.69, 46.53, 55.72, 55.97, 61.08, 69.82, 71.45, 111.30, 111.56, 113.00, 115.02, 120.67, 122.55, 129.00, 130.44, 145.02, 146.10, 147.38, 148.72, 178.83; IR (neat): 1517 (C=C), 1765 (C=O), 3420 (OH) cm^{-1}; MS (EI) *m/z* 402 (M^+); HRMS (EI): calcd for $C_{23}H_{28}O_6$: 402.1679 (M^+), found: 402.1671; $[\alpha]_D^{26}$ −19.7 (*c* 1.10, $CHCl_3$).

4.1.3. Synthesis of (−)-arctigenin derivatives 4g–4o

4.1.3.1. (4-Benzyloxy-3-methoxymethoxyphenyl)methanol (7). To a stirred solution of 4-benzyloxy-3-methoxymethoxybenzaldehyde (**6**) [14] (7.03 g, 25.8 mmol) in MeOH (50 mL) was added $NaBH_4$ (3.88 g, 103 mmol) at 0 °C, and the resulting mixture was stirred at room temperature for 2 h. The reaction was quenched with H_2O (50 mL), and the aqueous mixture was extracted with CH_2Cl_2 (50 mL × 3). The organic extracts were combined, dried over $MgSO_4$. The solvent was removed under reduced pressure, and the residue was chromatographed on silica gel (40 g, hexane:acetone = 3:1) to give **7** (6.66 g, 95%) as a pale yellow oil: ^{1}H NMR (300 MHz, $CDCl_3$) δ: 1.26 (1H, br), 3.53 (3H, s), 5.01 (2H, s), 5.16 (2H, s), 5.24 (2H, s), 6.88–6.96 (2H, m), 7.16 (1H, d, J = 1.9 Hz), 7.30–7.45 (5H, m); ^{13}C NMR (75 MHz, $CDCl_3$) δ: 56.13, 64.64, 70.88, 95.40, 114.25, 116.22, 121.06, 126.98, 127.61, 128.27, 134.16, 136.82, 146.60, 148.19; IR (neat): 1511 (C=C), 3419 (OH) cm^{-1}; MS (EI) *m/z* 274 (M^+); HRMS (EI): calcd for $C_{16}H_{18}O_4$: 274.1205 (M^+), found: 274.1188.

4.1.3.2. 2-(4-Benzyloxy-3-methoxymethoxybenzyl)malonic acid diethyl ester (8). To a stirred solution of **7** (711 mg, 2.59 mmol) in CH_2Cl_2 (26 mL) were added NEt_3 (0.43 mL, 3.11 mmol) and MsCl (0.22 mL, 2.85 mmol) at 0 °C, and the reaction mixture was stirred at room temperature for 0.5 h. The reaction was quenched with sat. $NaHCO_3$ (aq) (20 mL), and the organic layer was separated. The aqueous layer was extracted with CH_2Cl_2 (30 mL × 3), and the organic layer and extracts were combined, dried over $MgSO_4$. The